

1 Optimal HLA imputation of admixed population with dimension  
2 reduction

3 Venceslas Douillard<sup>1</sup>, Nayane dos Santos Brito Silva<sup>1,2</sup>, Sonia Bourguiba-Hachemi<sup>1</sup>,  
4 Michel S. Naslavsky<sup>3,4,5</sup>, Marilia O. Sclar<sup>3</sup>, Yeda A. O. Duarte<sup>6,7</sup>, Mayana Zatz<sup>3,4</sup>, Maria  
5 Rita Passos-Bueno<sup>3,4</sup>, Sophie Limou<sup>1</sup>, Pierre-Antoine Gourraud<sup>1</sup>, Élise Launay<sup>1,8</sup>, Erick C.  
6 Castelli<sup>2</sup>, Nicolas Vince<sup>1,\*</sup>, on behalf of the SNP-HLA Reference Consortium (SHLARC)

7 1. Nantes Université, INSERM, Ecole Centrale Nantes, Center for Research in Transplantation and  
8 Translational Immunology, UMR 1064, F-44000 Nantes, France.

9 2. São Paulo State University, Molecular Genetics and Bioinformatics Laboratory, School of Medicine,  
10 Botucatu, State of São Paulo, Brazil.

11 3. Human Genome and Stem Cell Research Center, University of São Paulo, São Paulo, SP Brazil

12 4. Department of Genetics and Evolutionary Biology, Biosciences Institute, University of São Paulo, São  
13 Paulo, SP Brazil

14 5. Hospital Israelita Albert Einstein, São Paulo, SP Brazil

15 6. Medical-Surgical Nursing Department, School of Nursing, University of São Paulo, São Paulo, SP Brazil

16 7. Epidemiology Department, Public Health School, University of São Paulo, São Paulo, SP Brazil

17 8. Department of Pediatrics and Pediatric Emergency, Hôpital Femme Enfant Adolescent, CHU de  
18 Nantes, Nantes, France.

19

20 License: CC-BY 4.0

21

22 Correspondence:

23 [nicolas.vince@univ-nantes.fr](mailto:nicolas.vince@univ-nantes.fr)

24 Nicolas Vince

25 Nantes Université, CR2TI UMR1064 – ITUN, CHU Nantes Hôtel Dieu, 30 bld Jean Monnet, 44093

26 Nantes Cedex 01, France, +33 2 40 08 74 24

27 <http://orcid.org/0000-0002-3767-6210>

28 Running title: Optimal HLA imputation of admixed population

29

30 **Abstract**

31 Human genomics has quickly evolved, powering genome-wide association studies (GWASs). SNP-based  
32 GWASs cannot capture the intense polymorphism of *HLA* genes, highly associated with disease  
33 susceptibility. There are methods to statistically impute *HLA* genotypes from SNP-genotypes data, but  
34 lack of diversity in reference panels hinders their performance. We evaluated the accuracy of the 1,000  
35 Genomes data as a reference panel for imputing HLA from admixed individuals of African and European  
36 ancestries, focusing on (a) the full dataset, (b) 10 replications from 6 populations, (c) 19 conditions for  
37 the custom reference panels. The full dataset outperformed smaller models, with a good F1-score of  
38 0.66 for *HLA-B*. However, custom models outperformed the multiethnic or population models of  
39 similar size (F1-scores up to 0.53, against up to 0.42). We demonstrated the importance of using  
40 genetically specific models for imputing admixed populations, which are currently underrepresented  
41 in public datasets, opening the door to HLA imputation for every genetic population.

42

43 **Introduction**

44 Genome-wide association studies (GWASs) have now become a strong ally in the understanding of the  
45 underlying mechanisms of diseases susceptibility and outcomes, with historical associations such as  
46 rs2395029 in HIV (Limou and Zagury 2013; Fellay et al. 2007), or the identification of 233 genomic  
47 regions linked to multiple sclerosis susceptibility (International Multiple Sclerosis Genetics Consortium  
48 2019). GWASs have also been performed as first lines of research at the beginning of the SARS-CoV-2  
49 outbreak to evaluate how host genetics can influence COVID-19 outcomes (Pairo-Castineira et al. 2021;  
50 COVID-19 Host Genetics Initiative 2021; Douillard et al. 2021b; Castelli et al. 2022). Starting from the  
51 first GWAS with hundreds of individuals in the 2000s (Klein et al. 2005; Duerr et al. 2006), multiple  
52 initiatives emerged in the last decade seeking to systematically gather clinical and genetic information,  
53 such as the UK Biobank (Bycroft et al. 2018), Japanese BioBank (Hirata et al. 2017), or TOPMed (Taliun  
54 et al. 2021), which count hundreds of thousands of samples. These studies greatly improved the  
55 comprehension of the genetic impact on phenotype variation (Visscher et al. 2017; Tam et al. 2019;  
56 Claussnitzer et al. 2020). Along with the collective organization effort, continuous advances in the  
57 domain of Single Nucleotide Polymorphism (SNP) imputation (Browning et al. 2018), and the  
58 availability of computing power from imputation servers, globally helped the genomics community  
59 (McCarthy et al. 2016).

60 A bystander effect of these GWASs has been confirming the central role of the Major  
61 Histocompatibility Complex (MHC), especially the *HLA* genes, in immune-related diseases. The MHC  
62 was discovered in the 1950s (Dausset 1958), and was identified as crucial for transplantation success  
63 (Dausset 1981). Association studies expanded our understanding of the role of MHC since 2.5% of all  
64 significant associations in the GWAS catalog (MacArthur et al. 2017) coincide with the MHC region,  
65 and approximately 20% of all traits are associated with at least one SNP within the MHC (Douillard et  
66 al. 2021b). The associations go from auto-immune diseases such as type 1 diabetes (Concannon et al.  
67 2009) or multiple sclerosis (International Multiple Sclerosis Genetics Consortium 2019), neurological

68 disorders such as Parkinson(Nalls et al. 2019), to infectious diseases such as HIV (Limou et al. 2009;  
69 Fellay et al. 2007), Hepatitis B (Hu et al. 2013) and C (Vergara et al. 2019).

70 In the context of genetic association studies, a parallel effort focused on direct association with *HLA*  
71 polymorphisms to understand the mechanisms in which HLA molecules impact disease susceptibility  
72 and severity. These studies have identified protective and risk *HLA* alleles, such as *HLA-DRB1\*15:01* in  
73 multiple sclerosis (Moutsianas et al. 2015), *HLA-DRB1\*09:01* with tIgE levels in asthma (Vince et al.  
74 2020b), specific HLA-DQB1 amino acids in hepatitis C virus infection (Valencia et al. 2022), or the HLA-  
75 DRB1 valine 11 in Parkinson's disease (Domenighetti et al. 2022), among many others. The five most  
76 polymorphic *HLA* genes (*HLA-A*, *HLA-B*, *HLA-C*, *HLA-DQB1*, and *HLA-DRB1*) are exceptionally diverse,  
77 with almost 30,000 alleles combined (Robinson et al. 2020). However, most of these alleles seem to  
78 have frequencies <1% (Maiers et al. 2007). Therefore, because of the high number of alleles and their  
79 low frequency, the HLA typing of thousands of individuals is necessary to reach sufficient statistical  
80 power for detecting associations. The cost-efficiency of directly typing *HLA* for such cohorts is limited.  
81 Thus, following the steps of the SNP association, the HLA community organized multiple typing  
82 initiatives and developed imputation tools (Meyer and Nunes 2017; Douillard et al. 2021a). The  
83 literature on HLA imputation articulates a dual focus on algorithms and reference data.

84 Regarding algorithms, several *HLA* imputation tools allow to create reference panels for imputing *HLA*  
85 alleles from SNP data: HIBAG (Zheng et al. 2014) and SNP2HLA (Jia et al. 2013) are the most common  
86 choices. Pappas et al. evaluated HIBAG to be the most accurate (Pappas et al. 2015). A new generation  
87 of software followed, with improvements to existing algorithms such as HLA\*IMP:03 (Motyer et al.  
88 2016) and CookHLA (Cook et al. 2021), or using deep learning with DEEP-HLA (Naito et al. 2021), all of  
89 which will probably gain traction over time. However, regarding reference datasets, the accuracy of  
90 *HLA* imputation results depends on the reference panel used to predict the target genotypes; if training  
91 and target data are not of the same ancestry, it will provide inaccurate results due to different HLA  
92 alleles and linkage disequilibrium patterns between SNP and HLA in different populations. To

93 circumvent this issue, researchers advocated for both: specific reference panels, such as in Japan  
94 (Okada et al. 2015), Finland (Ritari et al. 2020), or SweHLA (Nordin et al. 2020), and large multi-ethnic  
95 reference panels (Degenhardt et al. 2019; Luo et al. 2021). To pursue the different efforts, we created  
96 the SNP-HLA Reference Consortium, or SHLARC (Vince et al. 2020a). Our goal is to coordinate an  
97 international effort to gather HLA data and reference panels, make them available to the scientific  
98 community and improve the methodology of *HLA* association studies. Generally, *HLA* imputation is  
99 highly performant for European-origin populations as a large amount of data are available to build  
100 reference panels. Conversely, the challenge is higher when focusing on admixed or underrepresented  
101 populations as fewer data are available. A clear *HLA* imputation strategy remain to be defined to  
102 improve accuracy in these populations: here, we want to increase our understanding about *HLA*  
103 imputation performance between larger reference panels or smaller but customized (ancestry-  
104 matched) reference panels. Indeed, our hypothesis is that oversampling individuals for the reference  
105 panel with close genetic ancestry to the target individuals would increase accuracy for their specific  
106 *HLA* alleles. To explore this in our study, we focused on the results of *HLA* imputation on admixed  
107 populations using a multiethnic reference panel from the 1,000 Genomes Project (1KG), and  
108 investigating dimension reduction as a method to mitigate *HLA* imputation errors on rare alleles (1000  
109 Genomes Project Consortium et al. 2015; Byrska-Bishop et al. 2022).

110

111 **Results**

112 **HLA imputation strategy**

113 HLA imputation accuracy heavily depends on the data used as reference. Our study aims at finding the  
114 preferred *HLA* imputation combination of reference data selection and imputation method when  
115 dealing with a target population whose ancestry is absent or underrepresented in the available training  
116 data. The 1KG dataset presents a large diversity in populations as described in table S1 (1000 Genomes  
117 Project Consortium et al. 2015; Clarke et al. 2017), which can be grouped in 5 populations: African  
118 (AFR), American (AMR), European (EUR), East Asian (EAS), and South Asian (SAS). We selected these  
119 data as a training dataset to create 395 reference panels to be tested (Figure 1), including: (a) the full  
120 dataset (full1KG, N=2,504), (b) 10 replications from 6 populations (1KG, AFR, AMR, EUR, EAS, and SAS;  
121 N=200 for each), (c) 19 conditions for the custom reference panels (further described in the next  
122 chapter; 200<N<485); each condition replicated 5 times for each *HLA* gene (*HLA-A*, *HLA-B*, *HLA-C*, *HLA-*

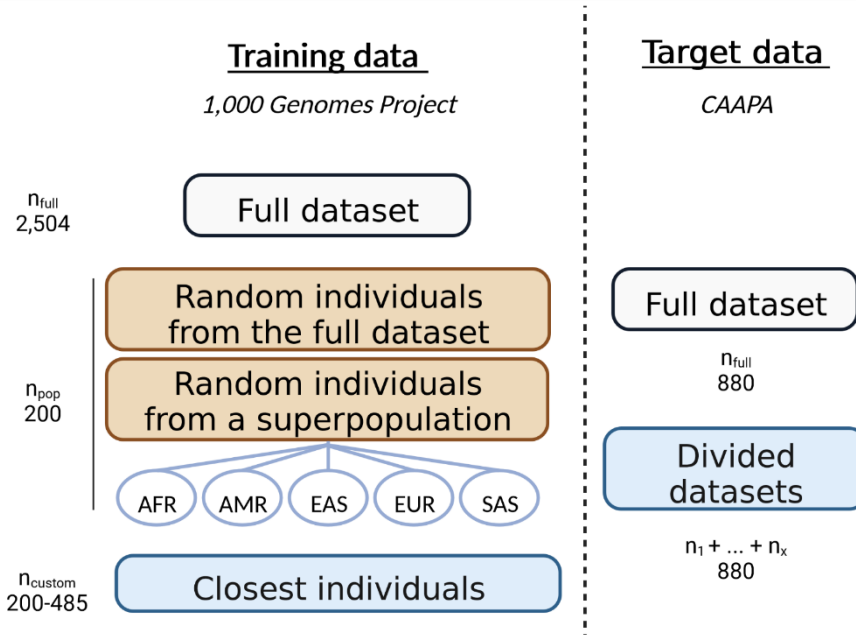


Figure 1 Selection strategy: description of the dataset selection for training and testing. Different subsets of the 1KG dataset are used as reference, selected by super-population or from genetic proximity with the CAAPA dataset. The HLA genotypes from CAAPA are either imputed from a single model or by multiple models specific to subsets of CAAPA.

123 *DQB1*, and *HLA-DRB1*).

124 The CAAPA cohort (Consortium on Asthma among African-ancestry Populations in the Americas) is  
125 constituted of 880 individuals with SNPs of the *MHC* region and HLA genotypes. These individuals are  
126 from admixed African and European ancestry in various proportions (Vince et al. 2020b). Only a small  
127 fraction of these populations ancestries are represented in the 1KG dataset, so we also wanted to  
128 evaluate the impact of admixture in the imputation process and accuracy. Thus, the CAAPA population  
129 was alternatively considered a unique dataset of 880 individuals, or as multiple subsets of it, depending  
130 on the representation with dimension reduction methods.

131 *Data selection for customized HLA imputation*

132 We created models with individuals from 1KG genetically close to the CAAPA target data: the custom  
133 models. We decided to rely on dimension reduction, common in population genetics, to assess  
134 individuals ancestry. The goal is to select 200 individuals from 1KG closest to the target data, regardless  
135 of their designated ancestry. Classically, ancestry is assessed with whole-genome SNPs by Principal  
136 Component Analysis (PCA). However, since we focused our study on HLA, we decided to represent the  
137 populations using only SNPs within the MHC region (29-34Mb from chr6). This representation strategy  
138 separated the African population and a portion of the American population in one part, and the rest  
139 of 1KG on the other (Figure 2A). The usual granularity of PCA on whole-genome genotypes (Figure S1A)  
140 is not obtained and does not allow grouping ancestries. However, we could identify well-separated

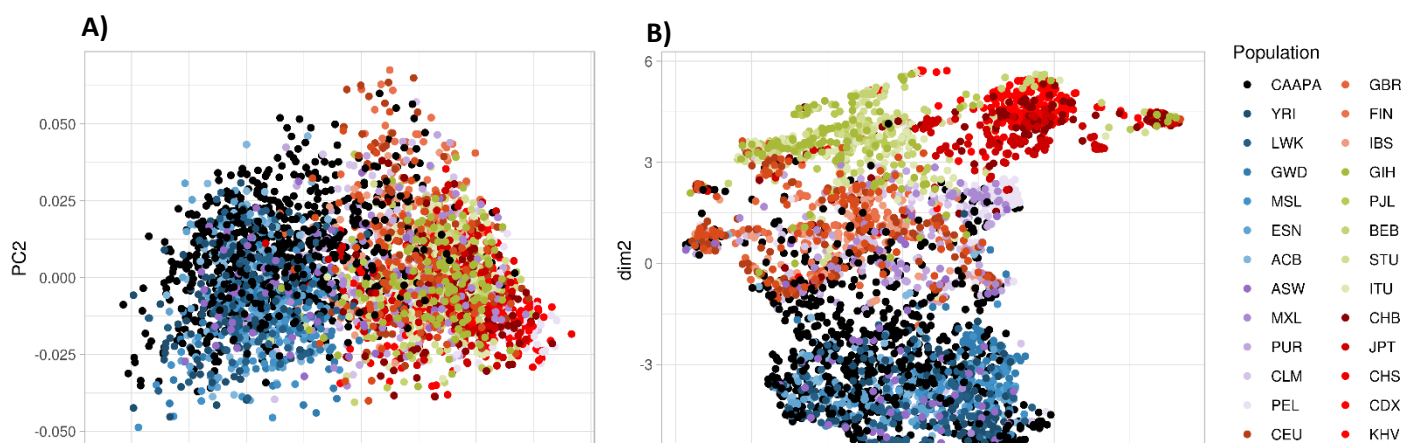


Figure 2 PCA (A) and UMAP (B) representation of 1KG and CAAPA dataset with merged genotypes of the MHC region. CAAPA is represented in black. Super-populations are colored in five main colors divided into different shades for each population (Table S1), including 5 super-populations: African (AFR) in blue, American (AMR) in purple, European (EUR) in orange, South Asian (SAS) in green, East Asian (EAS) in red. PCA does not separate well the population when restrained to the MHC region, whereas UMAP creates different groups of ancestries.

141 groups with a two-dimension UMAP (Uniform Manifold Approximation and Projection) of the MHC  
142 region (Figure 2B; UMAP on whole-genome genotypes in Figure S1B).

143 To investigate the effect of dimension reduction on HLA imputation, we tested 3 parameters for  
144 representation: the algorithm (PCA or UMAP), the number of dimensions used (2 or 10), and the  
145 genomic region covered by the genotypes dataset (the whole chromosome 6 or the MHC region, see  
146 also Figures S1). The different conditions are named after the combination of these parameters. For  
147 instance, a selection of the training data based on a UMAP using the distance computed in 10  
148 dimensions on every SNP available on chromosome 6 is named UMAPnonMHC\_10D.

149 We performed a silhouette score analysis to the resulting projection of the CAAPA dataset. We  
150 identified that, in every UMAP condition and with the ten-dimensions PCA in the MHC region, we could  
151 cluster CAAPA in more than one group. In these cases, we decided to create one model per group. We  
152 computed the average coordinates of the CAAPA individuals, then selected the 200 individuals from  
153 1KG closest to this point (Figure 3). To avoid redundant models, we checked the overlap of selected  
154 individuals between the conditions. Surprisingly, they all yielded a unique list of 1KG individuals, with  
155 low overlap between conditions (Figure S2). For the conditions where the CAAPA dataset was  
156 separated into different subsets, we imputed the individuals separately, thus relying on multiple  
157 models, but merged the results into one table. For example, with the two-dimension UMAP  
158 representation (genotypes from the MHC region), we computed three different models of 200 1KG  
159 individuals (Figure 3). We then imputed three CAAPA groups independently (357, 344, and 179  
160 individuals for a total of 880) and combined results into a unique table of imputation for the full  
161 dataset.

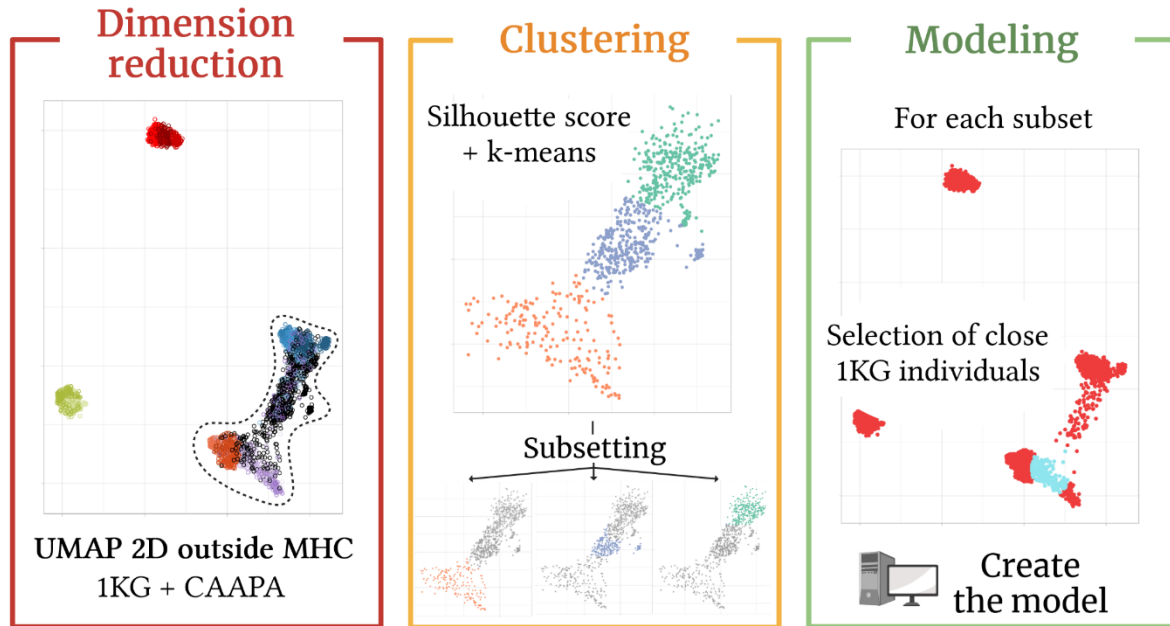
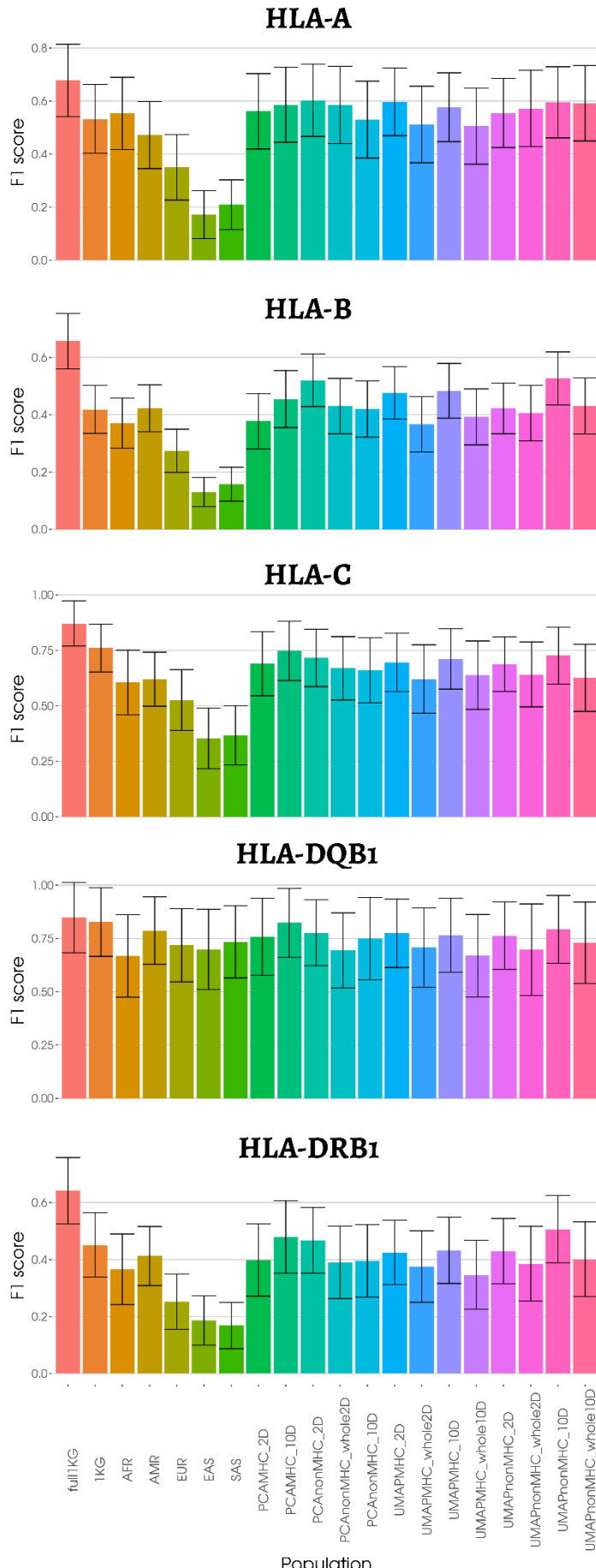


Figure 3 Creation of custom 1KG models for CAAPA imputation. 1) Dimension reduction allows the separation of individuals according to ancestry, using UMAP as an example. CAAPA is represented in black. Super-populations from 1KG are colored in five main colors: African (AFR) in blue, American (AMR) in purple, European (EUR) in orange, South Asian (SAS) in green, East Asian (EAS) in red. It is also possible to apply dimension reduction to one dataset and project another onto it. 2) Clustering of the target dataset: here CAAPA. The silhouette score allows to evaluate the preferred number of clusters, then k-means allows for subsetting. 3) Modeling. The barycenter of each cluster subset is computed, then 1KG individuals closest to this coordinate are selected (in light blue), allowing to create a custom model. Created with biorender.com

162 CAAPA HLA imputation comparison between usual and custom reference panels from 1KG data  
163 We have compared the different conditions by averaging the F1-score of each allele. As explained by  
164 Cook et al. (Cook et al. 2021), the F1-score has an advantage over other accuracy metrics for  
165 representing the rare alleles as it is the mean of two metrics, taking into account both the potential  
166 under- and over-prediction of an allele. As expected, the full1KG model (N=2,504) displayed the highest  
167 F1-score for all HLA genes, ranging from 0.64 for HLA-DRB1 to 0.87 for HLA-C (Figure 4). For HLA-B,  
168 full1KG has a score of 0.66. However, still for HLA-B, when considering the smaller models, we found  
169 that the 1KG models (F1-score of 0.42) and the populations with close ancestry to CAAPA (AFR: 0.37,  
170 AMR: 0.42) had nominally lower F1-score than some custom models (PCAnonMHC\_10D: 0.52,  
171 UMAPnonMHC\_10D: 0.53). This trend was also observed for HLA-A and HLA-DRB1, while HLA-C and  
172 HLA-DQB1 show a higher mean F1-score for the small 1KG models. F1-scores are not to be interpreted  
173 as regular accuracies. Indeed, when the same methodology is applied to compute the average

174    accuracies of each allele, these accuracies obtained more than 98% (represented as error rates in  
175    Figure S3). Additionally, the individual and haplotype accuracies, which corresponds to the proportion  
176    of correct genotypes (individuals can be counted as 0 or 1; incorrect vs. correct imputation) and the  
177    proportion of correct allele (individuals can be counted as 0, 0.5, or 1; incorrect vs. 1 correct allele vs.  
178    2 correct alleles imputation), respectively, also show values above 80% (Figure S4).



**Figure 4** Average F1-score of HLA allele predictions for HLA-A, HLA-B, HLA-C, HLA-DQB1, and HLA-DRB1 based on imputation of the CAAPA dataset, with different training models from the 1000 Genomes dataset. We have removed alleles that are not represented in the training datasets. Nomenclature of the models can be found in table S2. Full1KG, N=2,504. Small 1KG models (1KG, AFR, AMR, EUR, EAS, SAS), N=200. Custom models, 200< N <485.

180 To investigate the impact of custom models on imputation and why they seemed to perform better  
 181 for highly polymorphic genes, we stratified the mean F1-score metric by *HLA* allele frequency (Figure  
 182 5). The full1KG model (N=2,504) yielded a higher F1-score through all allelic frequencies. Custom  
 183 models performed equally or marginally better for the rarest alleles (frequency <= 0.1%) and the most

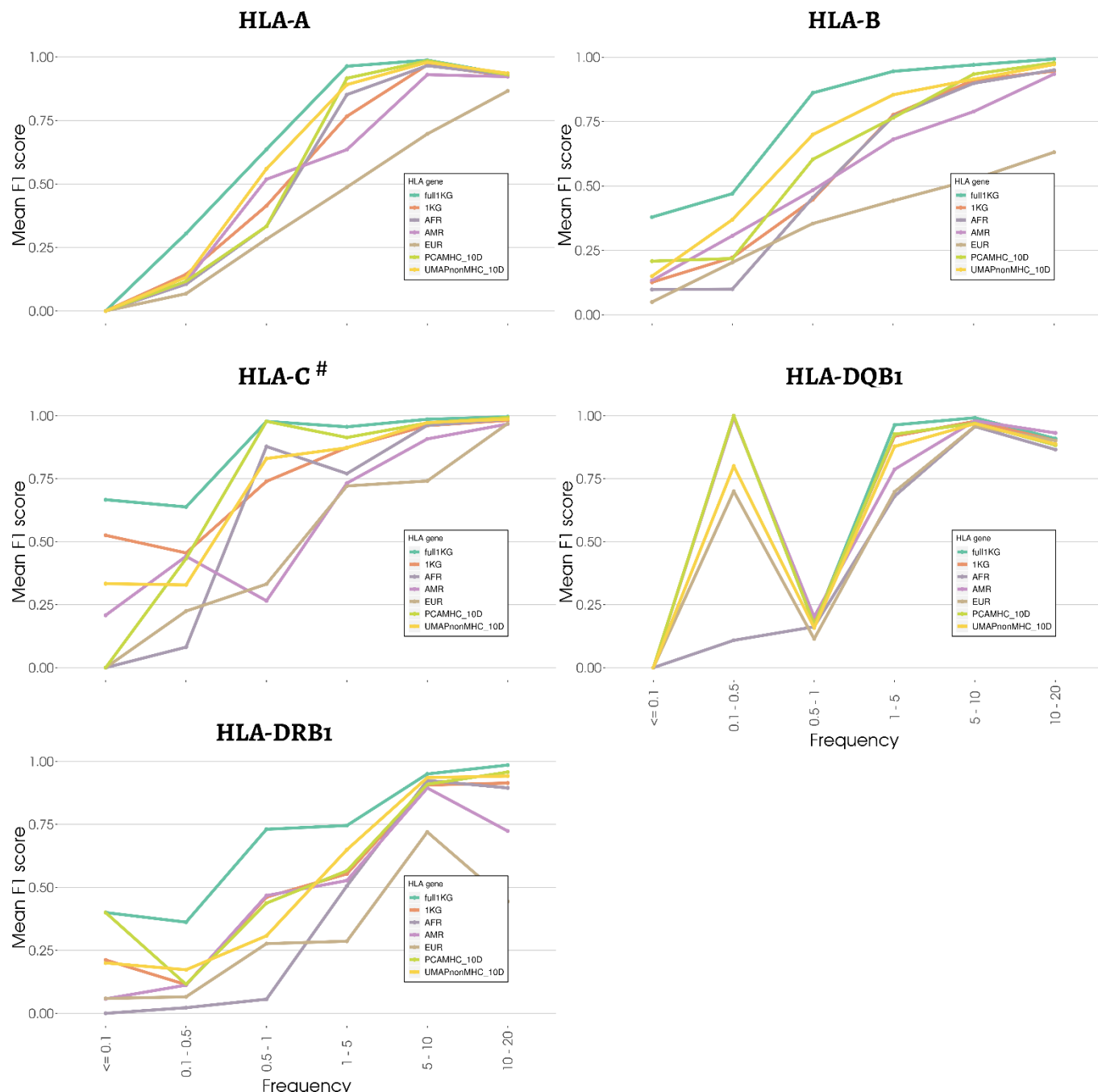


Figure 5 Mean F1-score of HLA alleles imputation, stratified by groups of frequency, for the full 1KG model, super-population models, and a selection of custom models. The custom models PCAMHC\_10D and UMAPnonMHC\_10D are displayed as they are the most accurate. #: HLA-C does not have the 10-20% frequency category. Therefore, unlike other genes, the last two categories correspond to 5-10% and >20%.

184 common alleles (frequency >10%). Still, they scored higher for every other category than population  
185 models. For *HLA-B*, UMAPnonMHC\_10D (N=485) presented an F1-score of 0.30, 0.70, 0.85, and 0.91  
186 for the categories from 0.1 to 10% frequency, whereas the multi-ethnic model (1KG, N=200) showed  
187 scores of 0.18, 0.45, 0.78, and 0.91. Notably, the reference panel based on the African population  
188 performed worse for *HLA-DQB1*. It can be explained by the allele *HLA-DQB1\*06:01*, which was  
189 represented only once and had an F1-score of 0.1.

190 The results showed that creating custom reference panels based on a genotypic distance between  
191 individuals can improve the outcome compared to multi-ethnic or declared ancestry panels. However,  
192 larger multi-ethnic reference panels are always more robust. We went further and looked directly at  
193 the imputation of *HLA* alleles individually.

194 When we analyzed results allele by allele, taking *HLA-A* (Figure 6) as an example, we observed that in  
195 most cases, custom models performed just as well, or a few points under the full dataset models (e.g.  
196 *HLA-A\*01:01*, *HLA-A\*23:01*). Several *HLA* alleles were better predicted with the custom models  
197 compared to the multi-ethnic (1KG) and population models (e.g. *HLA-A\*01:02*, *HLA-A\*80:01*),  
198 highlighting the importance of creating specific reference panels. We found cases where the full1KG  
199 model (N=2,504) or population models (N=200) were the only ones to predict the allele (e.g. *HLA-*  
200 *A\*02:06*, *HLA-A\*03:02*). However, we also found cases where custom models were the only ones to  
201 impute correctly the allele (e.g. *HLA-A\*02:04*). Zheng et al. (Zheng et al. 2014) showed that at least 10  
202 copies of an allele were needed in a model to be able to impute them. Nine *HLA-A* alleles were present  
203 in the training and target data but were not imputed by any of the models (e.g. *HLA-A\*02:11*, *HLA-*  
204 *A\*24:03*, *HLA-A\*26:08*). Often, the allele was present only in few individuals of the target data, causing  
205 the miscalled allele to weigh a lot in the score. We focused on *HLA-A* for visualization purposes, but  
206 the results applied to *HLA-B*, *HLA-C*, and *HLA-DRB1* (Figure S5). Interestingly for *HLA-DQB1*, the best  
207 custom models were never the best predictors. For most *HLA-DQB1* alleles, the best training dataset  
208 was the full1KG dataset. For *HLA-DQB1\*03:01*, however, the AMR and EUR super-populations yielded

209 better results. The different examples presented here show how a custom reference panel could help  
210 in the imputation of certain *HLA* alleles. However, since bigger models produce better imputation  
211 results overall, we would need to know when to select the results from the custom reference panel.

212 HLA imputation with HIBAG yields post-probabilities for each genotype. We tried to harness the few  
213 cases where custom models performed better (in terms of post-probabilities) to obtain hybrid  
214 imputation between the full models and the custom model. We chose UMAPnonMHC\_10D as it  
215 performed the best on multiple *HLA* genes. Unfortunately, the small number of samples in the custom  
216 models led to lower post-probabilities than the full model. In the few cases where UMAPnonMHC\_10D  
217 yielded better post-probabilities, the imputed genotype was not always correct, whereas the less likely  
218 genotype imputed by the other model was correct. In a real situation where the *HLA* alleles of the  
219 target data would not be known, there would be no way to choose between the imputed genotype of  
220 the two models (Figure S6).

221

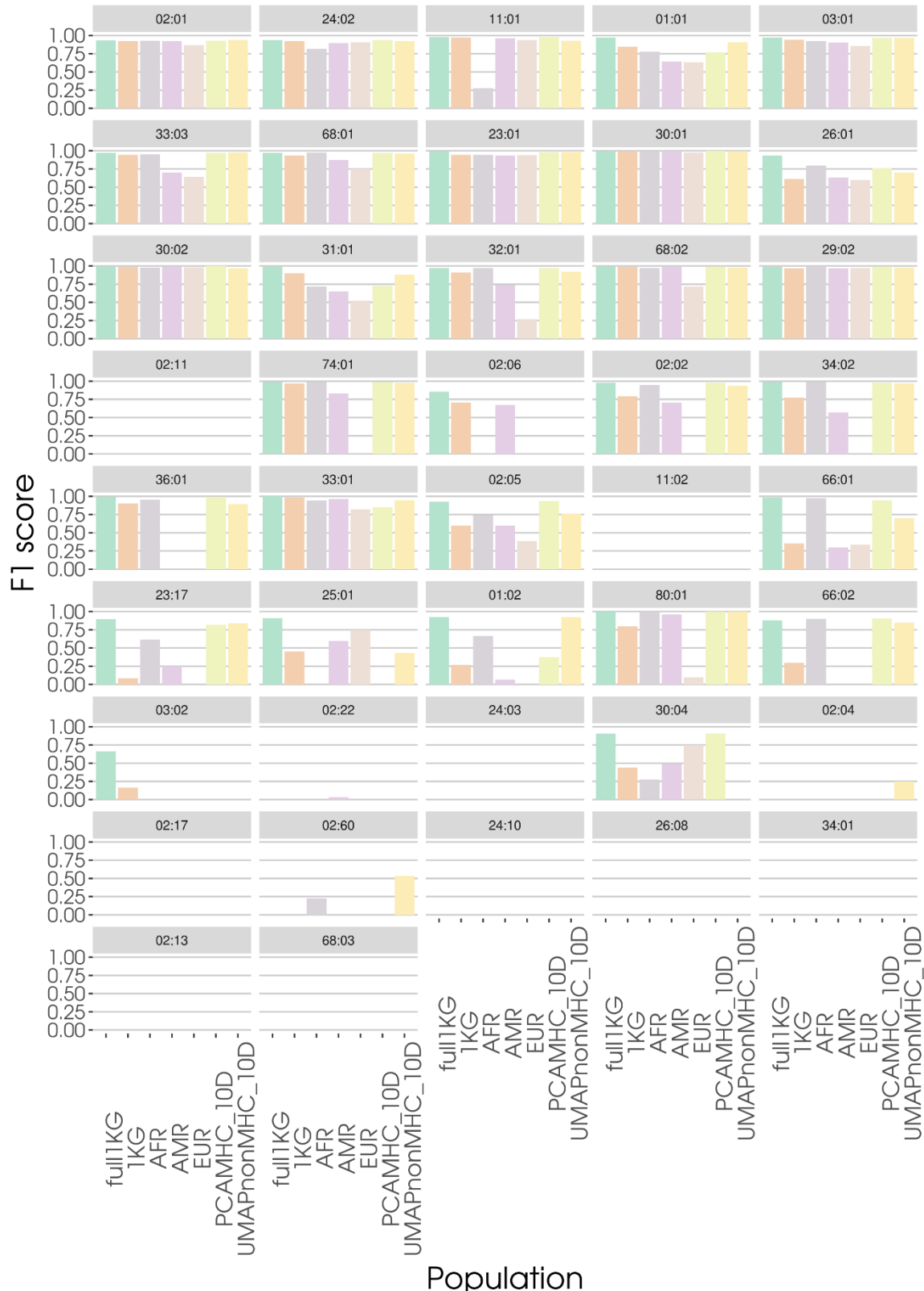


Figure 6 Mean F1-score of each HLA-A alleles (N=42) for the full 1KG training dataset, the African, American, European super-populations datasets, and the most accurate custom reference panels PCAMHC\_10D and UMAPnonMHC\_10D. Alleles are ordered by decreasing frequency in the 1KG dataset. Those absent from the training dataset have been removed to compute the means.

223 Replication with admixed Brazilian individuals from SABE  
 224 We replicated our methodology on another cohort of admixed individuals, the Longitudinal Health,  
 225 Well-Being, and Aging cohort (SABE - *Saúde, Bem-estar e Envelhecimento*) from Brazil, to validate the  
 226 impact of the models composition on *HLA* imputation (Figure 7). SABE is an independent dataset of  
 227 1,322 individuals from Brazil, mostly with European and African admixed ancestry (Naslavsky et al.  
 228 2022). To validate our conclusions, we used the same models as with the CAAPA dataset; therefore,  
 229 between 11.6% and 45.1% of the model SNPs were missing in the target data. Though it probably  
 230 reduced the imputation score overall, the missing SNPs were homogeneous across conditions for each  
 231 gene, with averages of 30.0% for *HLA-A*, 14.3% for *HLA-B*, 13.9% for *HLA-C*, 39.4% for *HLA-DQB1*, and

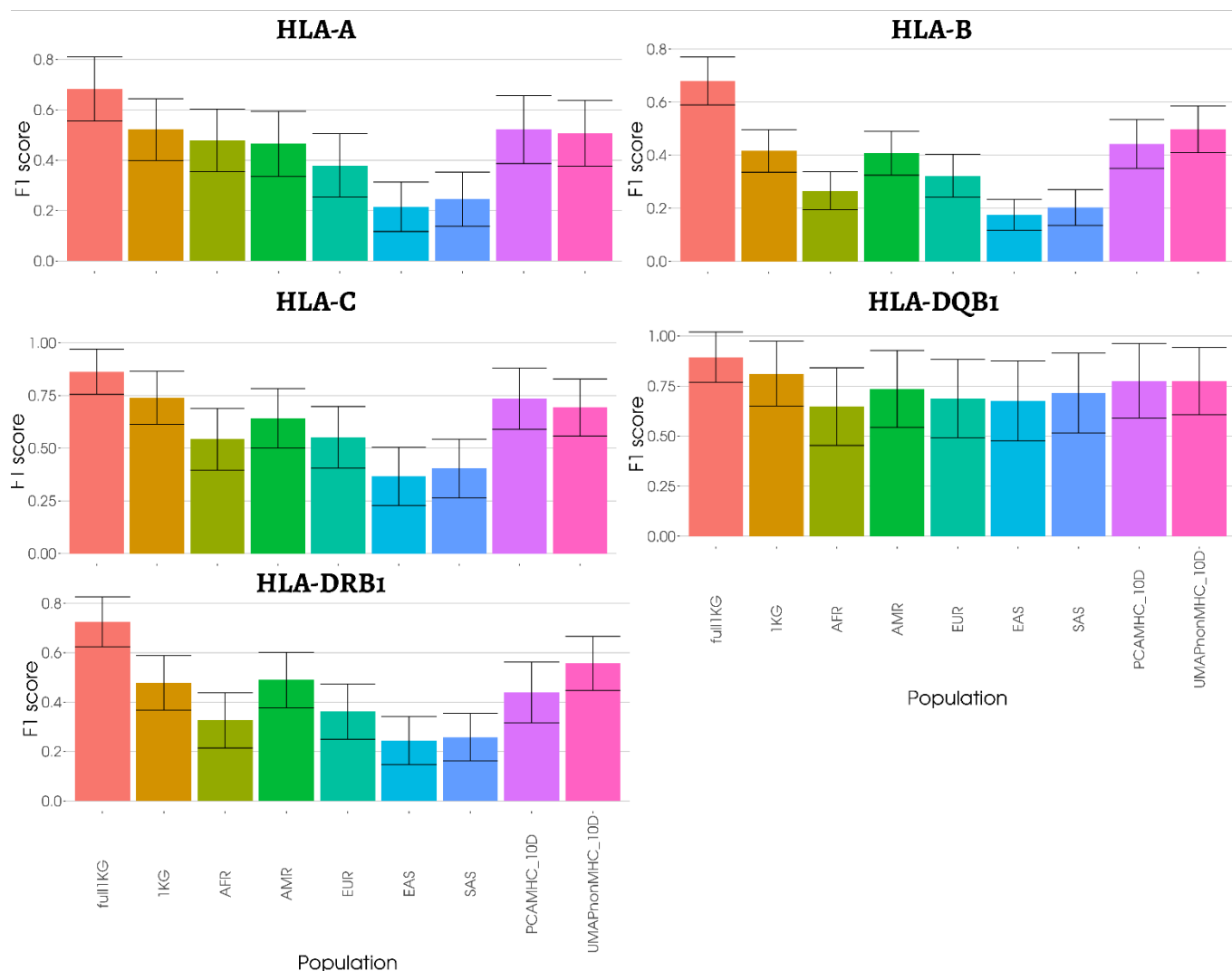


Figure 7 Mean F1-score of SABE's imputed *HLA-A*, *HLA-B*, *HLA-C*, *HLA-DQB1*, and *HLA-DRB1* genotypes, using the full 1KG model, compared to super-populations from 1KG or individual custom models selected by dimension reduction. Alleles absent from the training datasets were removed to obtain these values.

232 39,6% for *HLA-DRB1*. We also limited our study to the PCAMHC\_10D and UMAPnonMHC\_10D custom  
233 models, as these two models predicted *HLA-A*, *HLA-C*, *HLA-DQB1*, and *HLA-DRB1* better, out of all the  
234 custom models in the CAAPA dataset.

235 As with CAAPA, the custom models had nominally higher F1-score than the 1KG model, but only for  
236 the *HLA-B* (0.44, 0.50 for PCA and UMAP vs. 0.42 for 1KG) and *HLA-DRB1* (0.56 for UMAP vs. 0.48 for  
237 1KG). Overall, the validation with the SABE population showed the same patterns as the CAAPA  
238 population, with a global preference for the full1KG model and multiple cases where the custom  
239 reference panels were to be preferred but presented low post-probabilities genotypes.

240 **Discussion**

241 The HLA and immunogenetic community, along with the SHLARC (Vince et al. 2020a), carries a broad  
242 dynamic to provide scientists with reliable tools and reference panels for *HLA* imputation, thus  
243 increasing the power of *HLA* association studies to that of existing GWASs. We believe our results  
244 contribute to this effort. Our work focused on improving existing methods of *HLA* imputation by finely  
245 accounting for ancestry in the choice of the training model. Our underlying hypothesis was that  
246 oversampling individuals to create reference panels with close genetic ancestry compared to the target  
247 individuals would increase HLA imputation accuracy for rare *HLA* alleles. In this context, we chose to  
248 evaluate the imputation of CAAPA, an admixed African-American cohort, using reference panels  
249 composed of different combinations of 1,000 Genomes Project individuals: randomly selected from a  
250 population or selected for their estimated ancestry by dimension reduction. We showed that,  
251 ultimately, the number of individuals was the crucial point of HLA imputation. The reference panel  
252 composed of 2,504 individuals from 1KG systematically had a higher F1-score than other smaller  
253 models. Using fewer individuals for training by selecting individuals close to the ancestry of the target  
254 population was a good strategy and resulted in slightly better HLA imputation F1-scores, compared to  
255 multi-ethnic reference panels. The improvement did not concern the rarest or most common alleles,  
256 which are respectively badly and well imputed by all those models. At the allele level, we expected the  
257 full model to impute *HLA* alleles other models would not; we also saw the opposite with custom  
258 reference panels capturing a part of the information left out in the full model. Unfortunately, we could  
259 not conclude on its applicability since the custom reference panels had fewer individuals resulting in  
260 lower post-probabilities that rendered a hybrid imputation impossible. Research on SNP to SNP  
261 imputation also encounters the problem of lack of diversity for the imputation of rarer alleles, and are  
262 working with specific reference panels to enhance imputation accuracy (Kals et al. 2019; Herzig et al.  
263 2022).

264 Interestingly, we were also able to use UMAP for genomic ancestry representation, as can also be seen  
265 in recent research (Diaz-Papkovich et al. 2021; Sakaue et al. 2020; Dai et al. 2020). It presented a good

266 separation of ancestry groups in two dimensions when only using the MHC SNPs, concordant with the  
267 frequency difference of *HLA* alleles between populations (Maróstica et al. 2022). In contrast, PCA  
268 would fail to separate them in only two dimensions, limiting the possibility to visualize. PCA uses SNPs  
269 to explain most of the variance. Conversely, UMAP tries to preserve the topography of the higher  
270 dimensions in its reduction, taking into account every SNP available for distance. Besides, we observed  
271 a distance between individuals sometimes higher inside a labeled 1KG population than between  
272 populations, as described in Maróstica et al. (Lewontin 1972; Maróstica et al. 2022). This  
273 representation of this genomic diversity inside the MHC directly impacts how we should construct  
274 reference panels in the future and highlights the importance of gathering more data from different  
275 ancestry backgrounds.

276 Our work showed the potential interest of population-specific reference panels, as multiple studies  
277 have demonstrated (Okada et al. 2015; Ritari et al. 2020; Nordin et al. 2020; Luo et al. 2021; Mimori et  
278 al. 2019; Zhou et al. 2016; Nunes et al. 2016; Huang et al. 2020). However, we strayed further from the  
279 geographic definition of the population. We tried to find a local definition of ancestry to select training  
280 datasets. While doing so, we also omitted potential sides to the problem and created limits to our  
281 method. One important difference to *HLA* imputation compared to typing, inherent to the method, is  
282 the impossibility of predicting *de novo* alleles and the difficulty of imputing rare alleles. This issue is  
283 intrinsic to all training machine learning methods, and it is especially true for *HLA*, where each gene  
284 can have thousands of alleles. In HIBAG, for instance, an allele should be present at least 10 times in  
285 the training dataset to be predicted (Zheng et al. 2014). This study showed that this limit can be  
286 overcome to a certain extent but still hinders *HLA* imputation accuracy overall. Additionally, the choice  
287 to limit the number of randomly selected individuals was directly linked to the maximum of samples  
288 in the smallest population ( $n_{AMR}=347$ ). However, it has led to low imputation scores. Even though we  
289 performed replications, the difference between population models and the full dataset, or the custom  
290 models, may greatly vary if we increase this limit with another multi-ethnic dataset. It is one potential  
291 improvement to this work, which may validate or not our findings.

292 We chose to represent the *HLA* imputation with the F1-score, as seen in Cook et al. (Cook et al. 2021).  
293 This choice is convenient for the analysis of *HLA*, in which we encounter low and unbalanced  
294 frequencies between the different alleles. We set the F1-score at 0 when a specific allele was not  
295 imputed at all (whereas F1-score should be null) to represent all alleles in common between the two  
296 datasets and weigh this absence of imputation negatively. It has increased the confidence interval of  
297 each averaged F1-score and limited the possibility to find statistical differences between them. It is  
298 important to note that the F1-score gives a harsher view on *HLA* imputation because rare alleles have  
299 low scores, however, *HLA* imputation performs very well for common alleles (Figure S3) (Meyer and  
300 Nunes 2017).

301 Besides methodology, *HLA* imputation gains much accuracy from the number of samples and the  
302 diversity in the reference panels. This is why initiatives looking into expanding the *HLA* data and  
303 creating larger reference panels, such as Degenhardt et al., are essential to the field (Degenhardt et al.  
304 2019; Luo et al. 2021; Abi-Rached et al. 2018). With the SHLARC (Vince et al. 2020a), we advocate for  
305 the coordination of such efforts to provide multi-ethnic panels of sufficient size, and help researchers  
306 do *HLA* imputation to investigate *HLA* risk and protection alleles, focusing on the coverage of the globe  
307 for data gathering. The evolution of imputation tools will also consequently improve *HLA* imputation.  
308 HLA-IMP\*03 (Motyer et al. 2016) and CookHLA (Cook et al. 2021) showed improved results over the  
309 algorithms they are created upon, and DeepHLA (Naito et al. 2021) also showed high accuracy, with a  
310 specific focus on rare *HLA* alleles. Eventually, these efforts will reach a limit, and we think the main  
311 focus of research should be gathering data worldwide.

312 Our results demonstrated the interest of using genetically specific models for imputing admixed  
313 populations which are currently underrepresented, opening the door to *HLA* imputation for every  
314 genetic population, while also exemplifying some limitation. The SNP-HLA Reference Consortium  
315 (SHLARC) wants to contribute to the *HLA* association analysis community by providing a platform for  
316 *HLA* imputation with exhaustive and diverse reference panels. We hope this will help association

317 studies to rapidly increase their statistical power and become a natural extension of genome-wide

318 association studies pointing towards *HLA* association.

319

320 **Methods**

321 **Data description and processing**

322 SNPs data from the 1KG, CAAPA, and SABE cohorts were obtained from whole-genome sequencing.

323 The 1KG dataset is one of the most diverse public dataset with 2,504 individuals from 26 populations

324 (1000 Genomes Project Consortium et al. 2015; Clarke et al. 2017). These populations are grouped in

325 5 populations, as described in table S1: African (AFR), American (AMR), European (EUR), East Asian

326 (EAS), and South Asian (SAS). *HLA* genotyping for the *HLA-A*, *HLA-B*, *HLA-C*, *HLA-DQB1*, and *HLA-DRB1*

327 genes was published and made accessible using HLA calling algorithms for whole-genome sequencing

328 data (Abi-Rached et al. 2018). Moreover, the SNP data has been updated with a new whole-genome

329 sequencing of 30X coverage from the New York Genome Center (Byrska-Bishop et al. 2022). The CAAPA

330 cohort (Consortium on Asthma among African-ancestry Populations in the Americas) was created to

331 study asthma in African-ancestry populations. The aim of this study was to catalog genetic diversity in

332 these populations, especially the African Diaspora in the Americas. From this, we had access to 880

333 individuals with whole-genome sequencing data of the *MHC* region and HLA genotypes (Vince et al.

334 2020b). The *HLA* alleles were called with the Omixon software (Budapest, Hungary) from whole-

335 genome sequencing data (Vince et al. 2020b). The SABE (*Saúde, Bem-estar e Envelhecimento*) data

336 come from the longitudinal, census-based follow-up, Health, Well-Being, and Aging cohort of elderly

337 people from São Paulo, Brazil. SABE is an independent dataset of 1,322 admixed individuals from Brazil,

338 mostly with European and African admixed ancestry: details can be found in the whole-genome

339 sequencing flagship publication (Naslavsky et al. 2022). *HLA* genotypes for SABE cohort were obtained

340 after read alignment with hla-mapper 4.1. This application was designed to optimize the mapping of

341 *HLA* sequences produced by massively parallel sequencing procedures (Castelli et al. 2018); the

342 pipeline is available at [https://github.com/erickcastelli/HLA\\_genotyping/tree/main/version\\_2](https://github.com/erickcastelli/HLA_genotyping/tree/main/version_2).

343 SNPs data were handled with PLINK v1.90b6.21 (Chang et al. 2015) and went through the same quality

344 control step: the removal of A/T and G/C ambiguous SNPs, and SNPs with >2% missing genotypes and

345 <1% minor allele frequency. *HLA* data comprises two-field alleles for *HLA-A*, *HLA-B*, *HLA-C*, *HLA-DQB1*,  
346 and *HLA-DRB1*, stored in a CSV file. *HLA* imputation models were computed on R 3.5.3 (R Core Team  
347 2022) with HIBAG v1.19.3 (Zheng et al. 2014) and its complementary package HIBAG.gpu v0.9.1.  
348 Training data were subsetted with PLINK to contain only the SNPs present in the target data for CAAPA.

349 We limited the number of individuals within each reference panel to 200 to be able to compare the  
350 specific reference panels to the population reference panels. Indeed, this number is lower than the  
351 smallest population, allowing to resample the population and repeat the experiment.

### 352 [HLA imputation metrics](#)

353 We have evaluated imputation accuracy using the F1-score. The F1-score is a harmonic mean of  
354 sensitivity (for a specific allele, # of correctly predicted allele/# of said alleles in the target dataset) and  
355 the positive predictive value (for a specific allele, # of correctly predicted allele/# of predictions of said  
356 allele). This score has the property to give important weight to the coverage of a specific allele  
357 prediction. For instance, if a rare allele is present once in a dataset of 100 alleles and not predicted by  
358 the model, you would have a 99% accuracy but a F1-score of 0.

359 *HLA* imputation models are limited by the pool of *HLA* alleles in the training dataset and the SNPs  
360 available, contrary to *HLA*-typing software based on read alignment, which relies on the complete  
361 database of known *HLA* alleles and the assessment of all gene regions. Therefore, we chose to average  
362 the results of all alleles present in the training and target datasets. Additionally, if one of these alleles  
363 is not predicted by the model, the positive predictive value, by definition, cannot be computed; in this  
364 case, the F1-score is also null. Since we wanted to focus our analysis on rare alleles, we decided to set  
365 the F1 scores of such alleles to 0, to visualize the impact of *HLA* alleles that are in the training dataset  
366 but do not manage to impute the ones in the target data.

### 367 [Dimension reduction](#)

368 Principal Component Analysis (PCA) is routinely used in population genomics and association studies  
369 to study population ancestry. It relies on SNPs which are attributed to different contributions,

370 maximizing the variance in their genotypes. It allows separating populations along multiple orthogonal  
371 axes with different contributions for each SNP. Uniform Manifold Approximation Projection (UMAP)  
372 and t-SNE are central in single-cell transcriptomics analyses (McInnes et al. 2018; Becht et al. 2018).  
373 Recently, It has also appeared in population genomics publications (Diaz-Papkovich et al. 2021; Sakaue  
374 et al. 2020). UMAP is based on simplicial topology to identify sets of neighbors for each individual and  
375 try to preserve them while transforming coordinates into new ones with less dimensions.

376 We performed dimension reduction after merging 1KG and CAAPA data. We ran PCA with PLINK, and  
377 UMAP on the BiRD cluster from Nantes University, using the `umap` R package. This package does not  
378 handle missing data; therefore, we applied the PLINK geno filter with a 0 threshold beforehand to  
379 remove any SNP with missing data. We followed the same process with SABE but merged the dataset  
380 with both 1KG and CAAPA.

381 We applied a silhouette score on the coordinates of the CAAPA individuals to identify the preferred  
382 number of clusters. We then performed k-means with the number of clusters that had the highest  
383 silhouette score. If the maximum score was inferior to 0.4, we chose not to perform clustering because  
384 simulations showed different groups would overlap greatly.

385

386 [Data access](#)

387 1,000 Genomes SNP genotypes were retrieved from the International Genome Sample Resource (IGSR)  
388 and can be accessed through (<https://www.internationalgenome.org/data-portal/data-collection/30x-grch38>). 1,000 Genomes HLA genotypes of 2,693 individuals were recovered from Abi-  
390 Rached *et al.* (2018) at <https://doi.org/10.1371/journal.pone.0206512.s010>.

391 CAAPA SNPs were retrieved from the WGS data deposited in dbGAP with the accession code  
392 phs001123.v2.p1, described in Mathias, R. A. *et al.* (2016). CAAPA HLA genotypes were obtained with  
393 the Omixon software as described in <https://doi.org/10.1016/j.jaci.2020.01.011>.

394 For SABE, individual-level sequence datasets (BAM files) are available at the European Genome-  
395 phenome Archive (EGA), under EGA Study accession number EGAS00001005052. Further information  
396 about EGA can be found on <https://ega-archive.org>.

397 [Competing interest statement](#)

398 The authors declare that there are no competing interests.

399 [Acknowledgements](#)

400 We would like to thank the Centre de Calcul Intensif des Pays de la Loire. This work was supported by  
401 de Nantes Métropole, Région des Pays de la Loire and European Union (FEDER) via the Programme  
402 d'investissements d'Avenir (NExT, SHLARC Project, Nantes Université), the ATIP-Avenir Inserm  
403 program, the Région Pays de Loire ConnectTalent. Venceslas Douillard has received funding from the  
404 Inserm and Région Pays de la Loire. Nicolas Vince has received funding from the European Union's  
405 Horizon 2020 research and innovation program under the Marie Skłodowska-Curie grant agreement  
406 No. 846520. Funding was provided by The São Paulo Research Foundation (FAPESP) grants and  
407 fellowships (CEPID 2013/08028-1, SABE 2014/50649-6, INCT 2014/50931-3, 2013/17084-2,  
408 2017/19223-0, 2012/24731-1, 2018/15579-8, 2015/25020-0, 2020/02413-4) and Conselho Nacional  
409 de Desenvolvimento Científico e Tecnológico (CNPq INCT 465355/2014-5). The grant 2013/17084-2

410 supported creating and maintaining the hla-mapper software and the pipeline from HLA calling from

411 NGS data.

412

413 [References](#)

- 414 1000 Genomes Project Consortium, Auton A, Brooks LD, Durbin RM, Garrison EP, Kang HM, Korbel  
415 JO, Marchini JL, McCarthy S, McVean GA, et al. 2015. A global reference for human genetic  
416 variation. *Nature* **526**: 68–74.
- 417 Abi-Rached L, Gouret P, Yeh J-H, Di Cristofaro J, Pontarotti P, Picard C, Paganini J. 2018. Immune  
418 diversity sheds light on missing variation in worldwide genetic diversity panels. *PLoS ONE* **13**:  
419 e0206512.
- 420 Becht E, McInnes L, Healy J, Dutertre C-A, Kwok IWH, Ng LG, Ginhoux F, Newell EW. 2018.  
421 Dimensionality reduction for visualizing single-cell data using UMAP. *Nat Biotechnol.*
- 422 Browning BL, Zhou Y, Browning SR. 2018. A One-Penny Imputed Genome from Next-Generation  
423 Reference Panels. *Am J Hum Genet* **103**: 338–348.
- 424 Bycroft C, Freeman C, Petkova D, Band G, Elliott LT, Sharp K, Motyer A, Vukcevic D, Delaneau O,  
425 O’Connell J, et al. 2018. The UK Biobank resource with deep phenotyping and genomic data.  
426 *Nature* **562**: 203–209.
- 427 Byrska-Bishop M, Evani US, Zhao X, Basile AO, Abel HJ, Regier AA, Corvelo A, Clarke WE, Musunuri R,  
428 Nagulapalli K, et al. 2022. High-coverage whole-genome sequencing of the expanded 1000  
429 Genomes Project cohort including 602 trios. *Cell* **185**: 3426–3440.e19.
- 430 Castelli EC, de Castro MV, Naslavsky MS, Scliar MO, Silva NSB, Pereira RN, Ciriaco VAO, Castro CFB,  
431 Mendes-Junior CT, Silveira E de S, et al. 2022. MUC22, HLA-A, and HLA-DOB variants and  
432 COVID-19 in resilient super-agers from Brazil. *Front Immunol* **13**: 975918.
- 433 Castelli EC, Paz MA, Souza AS, Ramalho J, Mendes-Junior CT. 2018. Hla-mapper: An application to  
434 optimize the mapping of HLA sequences produced by massively parallel sequencing  
435 procedures. *Hum Immunol* **79**: 678–684.
- 436 Chang CC, Chow CC, Tellier LC, Vattikuti S, Purcell SM, Lee JJ. 2015. Second-generation PLINK: rising  
437 to the challenge of larger and richer datasets. *Gigascience* **4**: 7.
- 438 Clarke L, Fairley S, Zheng-Bradley X, Streeter I, Perry E, Lowy E, Tassé A-M, Flicek P. 2017. The  
439 international Genome sample resource (IGSR): A worldwide collection of genome variation  
440 incorporating the 1000 Genomes Project data. *Nucleic Acids Res* **45**: D854–D859.
- 441 Claussnitzer M, Cho JH, Collins R, Cox NJ, Dermitzakis ET, Hurles ME, Kathiresan S, Kenny EE, Lindgren  
442 CM, MacArthur DG, et al. 2020. A brief history of human disease genetics. *Nature* **577**: 179–  
443 189.
- 444 Concannon P, Chen W-M, Julier C, Morahan G, Akolkar B, Erlich HA, Hilner JE, Nerup J, Nierras C,  
445 Pociot F, et al. 2009. Genome-wide scan for linkage to type 1 diabetes in 2,496 multiplex  
446 families from the Type 1 Diabetes Genetics Consortium. *Diabetes* **58**: 1018–1022.
- 447 Cook S, Choi W, Lim H, Luo Y, Kim K, Jia X, Raychaudhuri S, Han B. 2021. Accurate imputation of  
448 human leukocyte antigens with CookHLA. *Nat Commun* **12**: 1264.
- 449 COVID-19 Host Genetics Initiative. 2021. Mapping the human genetic architecture of COVID-19.  
450 *Nature* **600**: 472–477.

- 451 Dai CL, Vazifeh MM, Yeang C-H, Tachet R, Wells RS, Vilar MG, Daly MJ, Ratti C, Martin AR. 2020.  
452 Population Histories of the United States Revealed through Fine-Scale Migration and  
453 Haplotype Analysis. *Am J Hum Genet* **106**: 371–388.
- 454 Dausset J. 1958. [Iso-leuko-antibodies]. *Acta Haematol* **20**: 156–166.
- 455 Dausset J. 1981. The major histocompatibility complex in man. *Science* **213**: 1469–1474.
- 456 Degenhardt F, Wendorff M, Wittig M, Ellinghaus E, Datta LW, Schembri J, Ng SC, Rosati E, Hübenthal  
457 M, Ellinghaus D, et al. 2019. Construction and benchmarking of a multi-ethnic reference  
458 panel for the imputation of HLA class I and II alleles. *Hum Mol Genet* **28**: 2078–2092.
- 459 Diaz-Papkovich A, Anderson-Trocmé L, Gravel S. 2021. A review of UMAP in population genetics. *J  
460 Hum Genet* **66**: 85–91.
- 461 Domenighetti C, Douillard V, Sugier P-E, Sreelatha AAK, Schulte C, Grover S, May P, Bobbili DR,  
462 Radivojkov-Blagojevic M, Lichtner P, et al. 2022. The Interaction between HLA-DRB1 and  
463 Smoking in Parkinson’s Disease Revisited. *Mov Disord*.
- 464 Douillard V, Castelli EC, Mack SJ, Hollenbach JA, Gourraud P-A, Vince N, Limou S. 2021a. Approaching  
465 Genetics Through the MHC Lens: Tools and Methods for HLA Research. *Front Genet* **12**:  
466 774916.
- 467 Douillard V, Castelli EC, Mack SJ, Hollenbach JA, Gourraud P-A, Vince N, Limou S, Covid-19, HLA &  
468 Immunogenetics Consortium and the SNP-HLA Reference Consortium. 2021b. Current HLA  
469 Investigations on SARS-CoV-2 and Perspectives. *Front Genet* **12**: 774922.
- 470 Duerr RH, Taylor KD, Brant SR, Rioux JD, Silverberg MS, Daly MJ, Steinhart AH, Abraham C, Regueiro  
471 M, Griffiths A, et al. 2006. A genome-wide association study identifies IL23R as an  
472 inflammatory bowel disease gene. *Science* **314**: 1461–1463.
- 473 Fellay J, Shianna KV, Ge D, Colombo S, Ledergerber B, Weale M, Zhang K, Gumbs C, Castagna A,  
474 Cossarizza A, et al. 2007. A whole-genome association study of major determinants for host  
475 control of HIV-1. *Science* **317**: 944–947.
- 476 Herzig AF, Velo-Suárez L, Frex Consortium, FranceGenRef Consortium, Dina C, Redon R, Deleuze J-F,  
477 Génin E. 2022. *Can imputation in a European country be improved by local reference panels?  
478 The example of France*. *Genetics* <http://biorxiv.org/lookup/doi/10.1101/2022.02.17.480829>  
479 (Accessed February 27, 2023).
- 480 Hirata M, Kamatani Y, Nagai A, Kiyohara Y, Ninomiya T, Tamakoshi A, Yamagata Z, Kubo M, Muto K,  
481 Mushirosa T, et al. 2017. Cross-sectional analysis of BioBank Japan clinical data: A large  
482 cohort of 200,000 patients with 47 common diseases. *J Epidemiol* **27**: S9–S21.
- 483 Hu Z, Liu Y, Zhai X, Dai J, Jin G, Wang L, Zhu L, Yang Y, Liu J, Chu M, et al. 2013. New loci associated  
484 with chronic hepatitis B virus infection in Han Chinese. *Nat Genet* **45**: 1499–1503.
- 485 Huang Y-H, Khor S-S, Zheng X, Chen H-Y, Chang Y-H, Chu H-W, Wu P-E, Lin Y-J, Liao S-F, Shen C-Y, et  
486 al. 2020. A high-resolution HLA imputation system for the Taiwanese population: a study of  
487 the Taiwan Biobank. *Pharmacogenomics J*.
- 488 International Multiple Sclerosis Genetics Consortium. 2019. Multiple sclerosis genomic map  
489 implicates peripheral immune cells and microglia in susceptibility. *Science* **365**.

- 490 Jia X, Han B, Onengut-Gumuscu S, Chen W-M, Concannon PJ, Rich SS, Raychaudhuri S, de Bakker PIW.  
491 2013. Imputing amino acid polymorphisms in human leukocyte antigens. *PLoS ONE* **8**:  
492 e64683.
- 493 Kals M, Nikopensius T, Läll K, Pärn K, Tönis Sikka T, Suvisaari J, Salomaa V, Ripatti S, Palotie A,  
494 Metspalu A, et al. 2019. *Advantages of genotype imputation with ethnically matched*  
495 *reference panel for rare variant association analyses*. *Genomics*  
496 <http://biorxiv.org/lookup/doi/10.1101/579201> (Accessed February 27, 2023).
- 497 Klein RJ, Zeiss C, Chew EY, Tsai J-Y, Sackler RS, Haynes C, Henning AK, SanGiovanni JP, Mane SM,  
498 Mayne ST, et al. 2005. Complement factor H polymorphism in age-related macular  
499 degeneration. *Science* **308**: 385–389.
- 500 Lewontin RC. 1972. The Apportionment of Human Diversity. In *Evolutionary Biology* (eds. T.  
501 Dobzhansky, M.K. Hecht, and W.C. Steere), pp. 381–398, Springer US, New York, NY  
502 [http://link.springer.com/10.1007/978-1-4684-9063-3\\_14](http://link.springer.com/10.1007/978-1-4684-9063-3_14) (Accessed February 27, 2023).
- 503 Limou S, Le Clerc S, Coulonges C, Carpentier W, Dina C, Delaneau O, Labib T, Taing L, Sladek R,  
504 Deveau C, et al. 2009. Genomewide association study of an AIDS-nonprogression cohort  
505 emphasizes the role played by HLA genes (ANRS Genomewide Association Study 02). *J Infect*  
506 *Dis* **199**: 419–426.
- 507 Limou S, Zagury J-F. 2013. Immunogenetics: Genome-Wide Association of Non-Progressive HIV and  
508 Viral Load Control: HLA Genes and Beyond. *Frontiers in Immunology* **4**: 1–13.
- 509 Luo Y, Kanai M, Choi W, Li X, Sakaue S, Yamamoto K, Ogawa K, Gutierrez-Arcelus M, Gregersen PK,  
510 Stuart PE, et al. 2021. A high-resolution HLA reference panel capturing global population  
511 diversity enables multi-ancestry fine-mapping in HIV host response. *Nat Genet* **53**: 1504–  
512 1516.
- 513 MacArthur J, Bowler E, Cerezo M, Gil L, Hall P, Hastings E, Junkins H, McMahon A, Milano A, Morales  
514 J, et al. 2017. The new NHGRI-EBI Catalog of published genome-wide association studies  
515 (GWAS Catalog). *Nucleic Acids Res* **45**: D896–D901.
- 516 Maiers M, Gragert L, Klitz W. 2007. High-resolution HLA alleles and haplotypes in the United States  
517 population. *Hum Immunol* **68**: 779–788.
- 518 Maróstica AS, Nunes K, Castelli EC, Silva NSB, Weir BS, Goudet J, Meyer D. 2022. How HLA diversity is  
519 apportioned: influence of selection and relevance to transplantation. *Philos Trans R Soc Lond*  
520 *B Biol Sci* **377**: 20200420.
- 521 McCarthy S, Das S, Kretzschmar W, Delaneau O, Wood AR, Teumer A, Kang HM, Fuchsberger C,  
522 Danecek P, Sharp K, et al. 2016. A reference panel of 64,976 haplotypes for genotype  
523 imputation. *Nat Genet* **48**: 1279–1283.
- 524 McInnes L, Healy J, Melville J. 2018. UMAP: Uniform Manifold Approximation and Projection for  
525 Dimension Reduction. <https://arxiv.org/abs/1802.03426> (Accessed February 27, 2023).
- 526 Meyer D, Nunes K. 2017. HLA imputation, what is it good for? *Hum Immunol* **78**: 239–241.
- 527 Mimori T, Yasuda J, Kuroki Y, Shibata TF, Katsuoka F, Saito S, Nariai N, Ono A, Nakai-Inagaki N,  
528 Misawa K, et al. 2019. Construction of full-length Japanese reference panel of class I HLA  
529 genes with single-molecule, real-time sequencing. *Pharmacogenomics J* **19**: 136–146.

- 530 Motyer A, Vukcevic D, Dilthey A, Donnelly P, McVean G, Leslie S. 2016. *Practical Use of Methods for*  
531 *Imputation of HLA Alleles from SNP Genotype Data*. Genetics  
532 <http://biorxiv.org/lookup/doi/10.1101/091009> (Accessed February 27, 2023).
- 533 Moutsianas L, Jostins L, Beecham AH, Dilthey AT, Xifara DK, Ban M, Shah TS, Patsopoulos NA,  
534 Alfredsson L, Anderson CA, et al. 2015. Class II HLA interactions modulate genetic risk for  
535 multiple sclerosis. *Nat Genet* **47**: 1107–1113.
- 536 Naito T, Suzuki K, Hirata J, Kamatani Y, Matsuda K, Toda T, Okada Y. 2021. A deep learning method  
537 for HLA imputation and trans-ethnic MHC fine-mapping of type 1 diabetes. *Nat Commun* **12**:  
538 1639.
- 539 Nalls MA, Blauwendraat C, Vallerga CL, Heilbron K, Bandres-Ciga S, Chang D, Tan M, Kia DA, Noyce AJ,  
540 Xue A, et al. 2019. Identification of novel risk loci, causal insights, and heritable risk for  
541 Parkinson's disease: a meta-analysis of genome-wide association studies. *Lancet Neurol* **18**:  
542 1091–1102.
- 543 Naslavsky MS, Sclar MO, Yamamoto GL, Wang JYT, Zverinova S, Karp T, Nunes K, Ceroni JRM, de  
544 Carvalho DL, da Silva Simões CE, et al. 2022. Whole-genome sequencing of 1,171 elderly  
545 admixed individuals from São Paulo, Brazil. *Nat Commun* **13**: 1004.
- 546 Nordin J, Ameur A, Lindblad-Toh K, Gyllensten U, Meadows JRS. 2020. SweHLA: the high confidence  
547 HLA typing bio-resource drawn from 1000 Swedish genomes. *Eur J Hum Genet* **28**: 627–635.
- 548 Nunes K, Zheng X, Torres M, Moraes ME, Piovezan BZ, Pontes GN, Kimura L, Carnavalli JEP, Mingroni  
549 Netto RC, Meyer D. 2016. HLA imputation in an admixed population: An assessment of the  
550 1000 Genomes data as a training set. *Hum Immunol* **77**: 307–312.
- 551 Okada Y, Momozawa Y, Ashikawa K, Kanai M, Matsuda K, Kamatani Y, Takahashi A, Kubo M. 2015.  
552 Construction of a population-specific HLA imputation reference panel and its application to  
553 Graves' disease risk in Japanese. *Nat Genet* **47**: 798–802.
- 554 Pairo-Castineira E, Clohisey S, Klaric L, Bretherick AD, Rawlik K, Pasko D, Walker S, Parkinson N,  
555 Fourman MH, Russell CD, et al. 2021. Genetic mechanisms of critical illness in COVID-19.  
556 *Nature* **591**: 92–98.
- 557 Pappas DJ, Tomich A, Garnier F, Marry E, Gourraud P-A. 2015. Comparison of high-resolution human  
558 leukocyte antigen haplotype frequencies in different ethnic groups: Consequences of  
559 sampling fluctuation and haplotype frequency distribution tail truncation. *Hum Immunol* **76**:  
560 374–380.
- 561 R Core Team. 2022. *R: A Language and Environment for Statistical Computing*. R Foundation for  
562 Statistical Computing, Vienna, Austria <https://www.R-project.org/>.
- 563 Ritari J, Hyvärinen K, Clancy J, FinnGen, Partanen J, Koskela S. 2020. Increasing accuracy of HLA  
564 imputation by a population-specific reference panel in a FinnGen biobank cohort. *NAR*  
565 *Genomics and Bioinformatics* **2**: lqaa030.
- 566 Robinson J, Barker DJ, Georgiou X, Cooper MA, Flück P, Marsh SGE. 2020. IPD-IMGT/HLA Database.  
567 *Nucleic Acids Res* **48**: D948–D955.

- 568 Sakae S, Hirata J, Kanai M, Suzuki K, Akiyama M, Lai Too C, Arayssi T, Hammoudeh M, Al Emadi S,  
569 Masri BK, et al. 2020. Dimensionality reduction reveals fine-scale structure in the Japanese  
570 population with consequences for polygenic risk prediction. *Nat Commun* **11**: 1569.
- 571 Taliun D, Harris DN, Kessler MD, Carlson J, Szpiech ZA, Torres R, Taliun SAG, Corvelo A, Gogarten SM,  
572 Kang HM, et al. 2021. Sequencing of 53,831 diverse genomes from the NHLBI TOPMed  
573 Program. *Nature* **590**: 290–299.
- 574 Tam V, Patel N, Turcotte M, Bossé Y, Paré G, Meyre D. 2019. Benefits and limitations of genome-wide  
575 association studies. *Nat Rev Genet* **20**: 467–484.
- 576 Valencia A, Vergara C, Thio CL, Vince N, Douillard V, Grifoni A, Cox AL, Johnson EO, Kral AH, Goedert  
577 JJ, et al. 2022. Trans-ancestral fine-mapping of MHC reveals key amino acids associated with  
578 spontaneous clearance of hepatitis C in HLA-DQ $\beta$ 1. *Am J Hum Genet* **109**: 299–310.
- 579 Vergara C, Thio CL, Johnson E, Kral AH, O'Brien TR, Goedert JJ, Mangia A, Piazzolla V, Mehta SH, Kirk  
580 GD, et al. 2019. Multi-Ancestry Genome-Wide Association Study of Spontaneous Clearance of  
581 Hepatitis C Virus. *Gastroenterology* **156**: 1496–1507.e7.
- 582 Vince N, Douillard V, Geffard E, Meyer D, Castelli EC, Mack SJ, Limou S, Gourraud P-A. 2020a. SNP-  
583 HLA Reference Consortium (SHLARC): HLA and SNP data sharing for promoting MHC-centric  
584 analyses in genomics. *Genet Epidemiol* **44**: 733–740.
- 585 Vince N, Limou S, Daya M, Morii W, Rafaels N, Geffard E, Douillard V, Walencik A, Boorgula MP,  
586 Chavan S, et al. 2020b. Association of HLA-DRB1\*09:01 with tIgE levels among African-  
587 ancestry individuals with asthma. *J Allergy Clin Immunol* **146**: 147–155.
- 588 Visscher PM, Wray NR, Zhang Q, Sklar P, McCarthy MI, Brown MA, Yang J. 2017. 10 Years of GWAS  
589 Discovery: Biology, Function, and Translation. *Am J Hum Genet* **101**: 5–22.
- 590 Zheng X, Shen J, Cox C, Wakefield JC, Ehm MG, Nelson MR, Weir BS. 2014. HIBAG--HLA genotype  
591 imputation with attribute bagging. *Pharmacogenomics J* **14**: 192–200.
- 592 Zhou F, Cao H, Zuo X, Zhang T, Zhang X, Liu X, Xu R, Chen G, Zhang Y, Zheng X, et al. 2016. Deep  
593 sequencing of the MHC region in the Chinese population contributes to studies of complex  
594 disease. *Nat Genet* **48**: 740–746.
- 595